



## Synthesis and Thermoluminescence of Novel $\text{Ag}_3\text{PO}_4:\text{Ba}^{2+}$ Nanophosphor as Gamma Radiations Detector



A. El-Adawy<sup>a</sup>, A. Hussein<sup>a</sup>, E.R. Sheha<sup>\*b</sup>, S. Abdel-Samad<sup>b</sup>, Ahmad A. Hassan<sup>c</sup>, M. Al-Abyad<sup>b</sup>

<sup>a</sup> Physics Department, Faculty of Science, Menoufia University, Egypt

<sup>b</sup> Nuclear physics department, Cyclotron Facility, Nuclear Research Center, Atomic Energy Authority, Egypt

<sup>c</sup> Metallurgy department, Nuclear Research Center, Atomic Energy Authority, Egypt.

### Abstract

$\text{Ba}^{2+}$  activated  $\text{Ag}_3\text{PO}_4$  ( $\text{APB}_6$ ) orthophosphate as novel synthetic nanophosphor material was prepared using different impurity concentrations (1, 3, 5, 6 and 7 wt%) of  $\text{BaCl}_2$  salt. Coprecipitation method was used in preparation. The prepared nanophosphors were characterized via X-Ray Diffraction (XRD) and High-Resolution Transmission Electron Microscopy (HR-TEM) and the results confirmed the existence of nanoparticles. The thermoluminescence (TL) properties of the samples were extensively studied, where the  $\text{APB}_6$  sample with 6 wt%  $\text{Ba}^{2+}$  showed considerable TL characteristics. All the studied samples were subjected to optimum thermal annealing of 500 °C for 1h and a heating rate of 5°C/s was applied. The TL response of  $\text{APB}_6$  nanophosphor exhibited the highest value in comparison with that of other compositions. In addition,  $\text{APB}_6$  sample revealed a good linearity of TL response within the gamma ray doses between 15 and 100 Gy, where a linear response is obtained with .0.9925 correlation coefficient. It also showed relationally low rate of fading of about 26% within a 50 days of storage. These good characteristics make the new prepared  $\text{APB}_6$  phosphor to be highly considered as a new potential TL dosimeter and can efficiently be used as  $\gamma$ -irradiation detector in many applications of ionizing radiation.

*Keywords: gamma rays, Nanophosphor. Ba, Glow curve, Dosimetry*

### 1. Introduction

In the present scientific world, ionizing radiation has been found very useful in engineering, medicine, science and technology. Professionals have worked in this direction, investigated and standardized many analytical methods to estimate the doses of radiation [1, 2]. During the last decades, there were extensive researches on the use of thermoluminescence detectors (TLDs) in the field of radiations dosimetry. Worldwide, there are different types of phosphor-based thermoluminescent dosimetric families widely being in use [3]. TLD has reached a great development and a high acceptance degree for dosimetry, among the international scientific community since the first works carried out by Daniels, Boyd and Saunders [4]. TL materials are formed in bulk, micro, and nanocrystal structures where the latter is always expected to have the most

favorable TL features than the others are [5]. TLDs have many successful diversified applications in radiation monitoring of environmental and radiation workers exposure [6,7]. The TL phenomenon is based on measuring the light emitted from irradiated phosphor materials after having been heated [8]. In the last few years, orthophosphates have found increasing interest for their potential applications in the field of scintillators, solid-state lighting and TLD [9-12]. In addition, they have good features such as high emission intensity, low effective atomic number, nontoxicity, good luminescent properties, low cost synthesis method and excellent thermal stability [13-15]. Currently, silver orthophosphate ( $\text{Ag}_3\text{PO}_4$ ) is an important host material for activator ions in their lattice due to its high chemical stability, high quantum yield and low sintering temperature [16-21]. Moreover, it has become a promising photocatalyst driven by visible light. Therefore, we will focus in

\*Corresponding author e-mail emad.sheha@eaea.org.eg.; (Emad R. Sheha).

Receive Date: 08 February 2021, Revise Date: 11 March 2021, Accept Date: 16 March 2021

DOI: 10.21608/EJCHEM.2012.62097.3335

©2021 National Information and Documentation Center (NIDOC)

this article on the progress of the study of  $\text{Ag}_3\text{PO}_4$  based dosimetric materials [22-25]. The work presented herein intended to synthesize and investigate the thermoluminescence properties of new inexpensive nanostructure systems of undoped  $\text{Ag}_3\text{PO}_4$  and barium activated silver orthophosphate ( $\text{APB}_6$ ) compounds. Furthermore, the effects of thermal annealing and dopant concentration on the TL characteristics of these synthesized samples were extensively studied to explore and assure the goodness of using such new prepared compounds as promising gamma dosimeters.

## 2. Experimental

### 2.1. Samples preparation

High purity  $\text{BaCl}_2$  (98.98%),  $\text{Ba}(\text{NO}_3)_2$  (99.96%)  $\text{AgNO}_3$  (99.98%),  $\text{Na}_2\text{HPO}_4$  (99.98%) and absolute ethanol, were used to fabricate the undoped and  $\text{Ba}^{2+}$  doped  $\text{Ag}_3\text{PO}_4$  nanoparticles compounds. The  $\text{Ag}_3\text{PO}_4$  nanoparticles (NPs) sample was synthesized by the coprecipitation method [26-28]. The preparation was done as in the following steps: an appropriate amount of ( $\text{AgNO}_3$ ) salt was dissolved completely in 50 ml of ethanol with stirring at room temperature. Then an equal amount of 0.2 M  $\text{Na}_2\text{HPO}_4$  solution was added slowly to the previous mixture under continuous magnetic stirring. As a result, a yellow precipitate was obtained, collected and washed many times with distilled (DI) water. The precipitate was then, dried at  $90^\circ\text{C}$  in an oven for overnight to finally obtain the  $\text{Ag}_3\text{PO}_4$  (AP) nanocrystalline sample to be ready for any use.

The  $\text{Ag}_3\text{PO}_4\text{:Ba}^{2+}$  (APB) nanocrystalline was synthesized at room temperature utilizing an environmental friendly coprecipitation technique. Different weight ratios of  $\text{BaCl}_2$  salt (1, 3, 5, 6 and 7%) donated as  $\text{APB}_1$ ,  $\text{APB}_3$ ,  $\text{APB}_5$ ,  $\text{APB}_6$  and  $\text{APB}_7\%$  were dissolved completely in appropriate solvent with stirring at room temperature. Then  $\text{Ba}^{2+}$  salt with different concentrations were added drop wise to the previous prepared solution (AP) under vigorous stirring at room temperature. After that, the white precipitate has been collected and washed with DI water. Then the white precipitate was dried at  $90^\circ\text{C}$  in an oven for overnight to finally obtain the APB nanoparticles to be ready for any use.

Many groups of  $\text{APB}_6$  samples were subjected to annealing process at different temperature 300, 400, 500, 600 and  $700^\circ\text{C}$  for one hour. Then, all the annealed samples at different temperature are arranged and irradiated to 100 Gy of gamma absorbed dose. After that the relation between TL intensity and annealing temperature were measured by TLD-Reader, then the optimum temperature degree, which has a high TL-intensity value was defined. The TL-response as a function of the temperatures has studied. Different batches of  $\text{APB}_6$  with optimum conditions have packed in lightproof capsule and irradiated to different gamma rays doses. After that, the characteristic glow curves of  $\text{APB}_6$  nanophosphor have recorded by the TLD-reader, and presented graphically.

### 2.2. Sample irradiation and measurement

Co-60 gamma cell CM-20 manufactured by Russia at Cyclotron Facility, Nuclear Research Center (NRC), Egyptian Atomic Energy Authority (EAEA) was used to irradiate the samples at different gamma doses from (15-100Gy). The prepared powder samples were packed in ependorf tubes and placed inside one of the irradiation chambers at a position located along the longitudinal axis to the sources. Then the irradiator activity was 1.4 kCi during the present experiments. The actual dose rate was 0.5 kGy/h, according to National Physical Laboratory (NPL) alanine reference dosimeter (ISO/ASTM 51261, 2004).

The X-ray diffraction (XRD) patterns of synthesized (AP) and ( $\text{APB}_6$ ) samples were obtained using X-ray diffractometer, Philips (PW/1710), with Ni filter and  $\text{Cu-K}\alpha$  radiation ( $\lambda=1.542 \text{ \AA}$ ). The X-ray tube was operated at 40 kV and 30 mA anode current. The two-theta degree sweep angle varied in the range  $20^\circ$ -  $80^\circ$  with step 0.02. The obtained (XRD) patterns were compared with the *Joint Council Powder Diffraction Data* (JCDPs) for standards. The nanostructures of the prepared (AP) and ( $\text{APB}_6$ ) phosphors were investigated using high-resolution transmission electron microscope (HR-TEM model JEM-2100, JEOL, Japan).

The TL glow curve measurements were carried out using TLD reader [model-1009I, Nucleonix system, India]. The TL glow curves have recorded by

taking affixed amount for each time with a linear heating temperature rate of 5 °C/s and preheating 20 °C until reach a maximum temperature up to 350 °C.

### 3. Results and discussion

#### 3.1. Thermoluminescence measurements

The pre-annealed (500 °C for 1h), 100 Gy gamma irradiated nanostructure of  $\text{Ag}_3\text{PO}_4$  (AP) did not showed any TL response. In addition, the TL measurements of  $\text{Ag}_3\text{PO}_4:\text{Ba}^{2+}$  (APB) were extensively done under different conditions. A detailed study will be followed up.

##### 3.1.1. Optimum co-host type of $\text{Ba}^{2+}$ salts

Two co-host types of  $\text{Ba}^{2+}$  salts  $\text{Ba}(\text{NO}_3)_2$ , and  $\text{BaCl}_2$  were individually used in preparation of APB nanophosphors samples. The two resulted samples were first annealed at 500°C for 1h, exposed to 100 Gy of  $\gamma$ -dose, and then their TL glow curves were measured at 5 °C/s heating rate as displayed in Fig. (1).

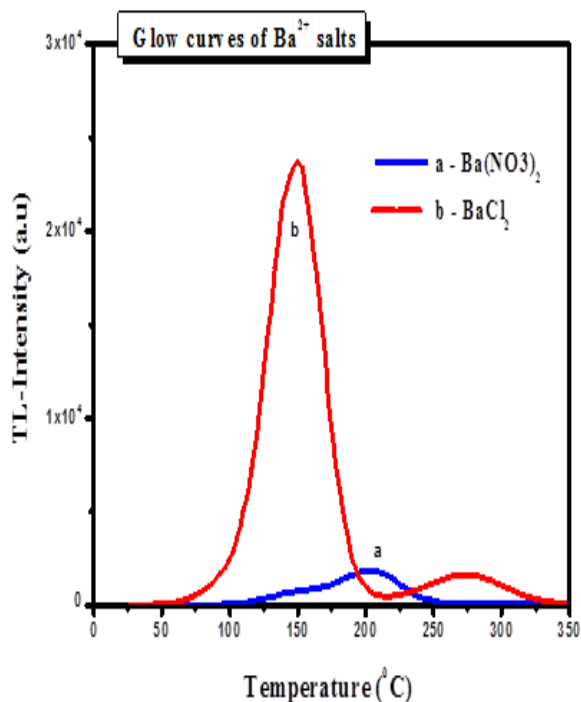


Fig. 1: TL glow curves of  $\text{Ag}_3\text{PO}_4:\text{Ba}^{2+}$  nanophosphors prepared with different of  $\text{Ba}^{2+}$  co-host types, exposed to 100 Gy  $\gamma$ -dose and recorded at 5°C/s.

By inspection of Fig. (1), we can notice that the shape, position, and TL intensity of the glow curves are strongly co-host type dependent. The APB

sample prepared from the  $\text{BaCl}_2$  salt exhibits the highest TL intensity than of the others. The TL intensity value of APB sample prepared from  $\text{BaCl}_2$  co-host salt is about 30 times higher than that obtained from  $\text{Ba}(\text{NO}_3)_2$  salt. Therefore, only APB nanostructure sample previously prepared using  $\text{BaCl}_2$  salt was consider in our investigations.

##### 3.1.2. Optimum $\text{Ba}^{2+}$ dopant concentration in APB nanophosphors.

Nanophosphors made of AP nanostructure samples activated with different  $\text{Ba}^{2+}$  weight ratios of 1, 3, 5, 6 and 7% were prepared and donated by APB<sub>1</sub>, APB<sub>3</sub>, APB<sub>5</sub>, APB<sub>6</sub> and APB<sub>7</sub> respectively. A coprecipitation method was used in the preparation with the  $\text{BaCl}_2$  co-host salt. Samples were first annealed at 500 °C for 1h, after that, exposed to 100 Gy of  $\gamma$ -dose. Fig. (2) shows the resulted glow curves of APB<sub>1</sub>, APB<sub>3</sub>, APB<sub>5</sub>, APB<sub>6</sub> and APB<sub>7</sub> samples recorded at 5 °C/s heating rate. All samples were first annealed at 500 °C for 1h and then exposed to 100 Gy of  $\gamma$ -dose.

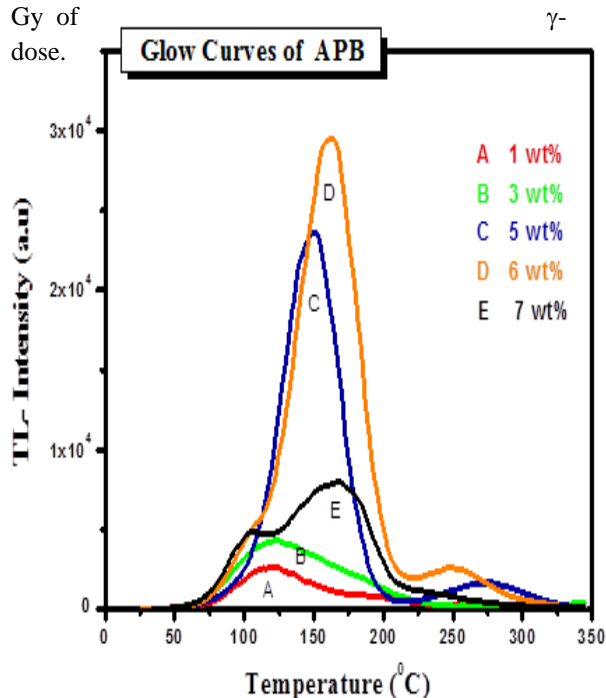


Fig. 2: The glow curves of  $\text{Ag}_3\text{PO}_4:\text{Ba}^{2+}$  nanophosphor having different impurity concentrations (1-7 wt%) and exposed to test dose 100Gy of  $\gamma$ -rays.

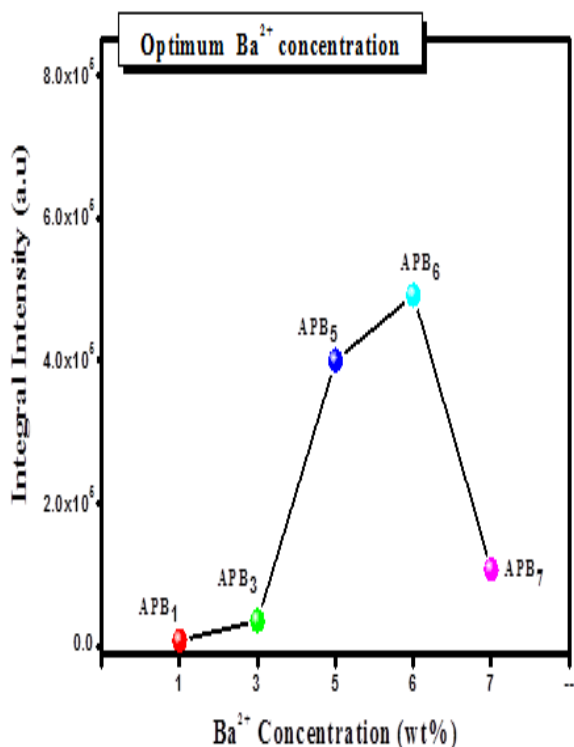


Fig. 3: Show the variation of TL intensity with the Ba<sup>2+</sup> concentrations, where maximum TL value was observed at 6 wt% concentration of optimal Ba<sup>2+</sup> salt.

Fig. (3), shows that the highest TL-response corresponded to 6 wt% Ba<sup>2+</sup> concentration. The TL-response of APB<sub>6</sub> was about 54, 14, 1.2 and 5 times higher than those of APB<sub>1</sub>, APB<sub>3</sub>, APB<sub>5</sub> and APB<sub>7</sub> samples, respectively. The decrease of TL-response values greater than 6 wt% can be attributed to the phenomenon of concentration quenching effect [29, 30]. Therefore, only APB<sub>6</sub> nanophosphor sample previously prepared using BaCl<sub>2</sub> co-host salt was selected for further investigations as given below.

### 3.1.3. Optimum annealing conditions of APB<sub>6</sub> nanophosphors

Different batches of APB<sub>6</sub> were subjected to isochronal annealing process at four different temperatures 300, 400, 500, 600 and 700 °C for a period of 1 h. Samples were then exposed to 100 Gy of gamma dose and the TL was recorded at 5°C/s heating rate. Fig. (4) exhibits the glow curves of APB<sub>6</sub> samples prepared at different annealing temperatures and Fig. (5) display the TL-point representations of data in Fig. (6).

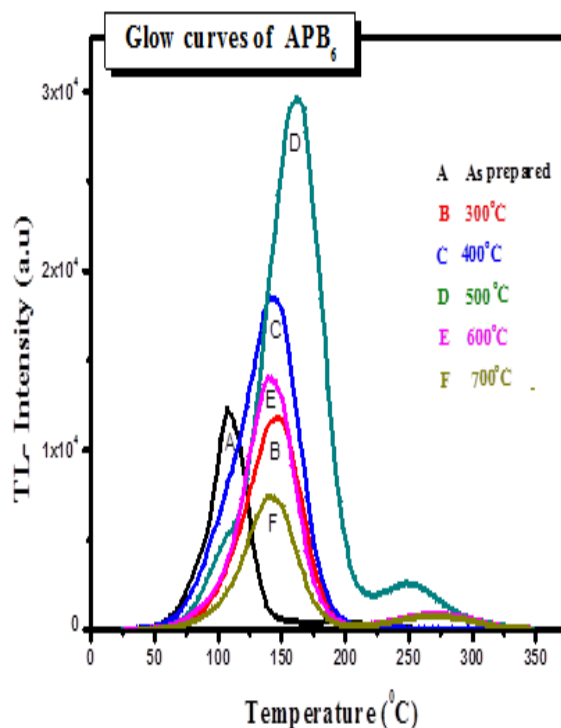


Fig. 4: TL glow curves of APB<sub>6</sub> nanophosphor annealed at different temperatures (300-700 °C/h) and exposed to 100 Gy of  $\gamma$ -dose

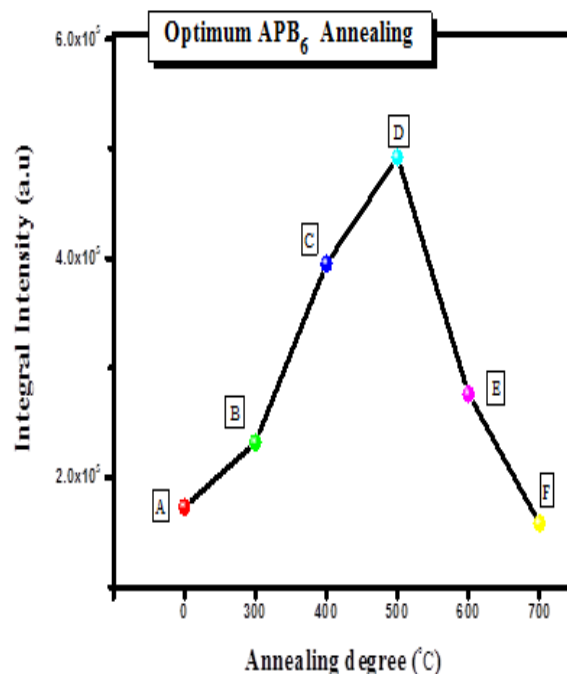


Fig. 5: The change of TL intensity with the annealing degree, and the optimum thermal annealing was observed at 600 °C/h.

From Fig. (4 and 5), it can be noticed that the best (optimum) annealing condition is found to be 600 °C for 1h. In summary, the optimum conditions of the present new prepared nanophosphors are (i) BaCl<sub>2</sub> as co-host salt (ii) 6 wt% (Ba<sup>2+</sup>) concentrations (iii) annealing at 500 °C for 1h. Eventually, the APB<sub>6</sub> sample is our best choice having maximum TL-response and better TL-glow curves temperature domain.

### 3.1.4. Glow curves of APB<sub>6</sub> at different Y-ray doses

The effect of different Y-ray dose on the glow curve of APB<sub>6</sub> sample was studied within a dose range from 15 to 100 Gy, recorded at 5 °C/s heating rate and given in Fig.(6). This figure shows that, the TL-intensity increases with increasing gamma dose and the glow curve are approximately similar in shape and position. This increasing in trapping centers, created by radiation, reflects such increase in TL-intensities with gamma doses

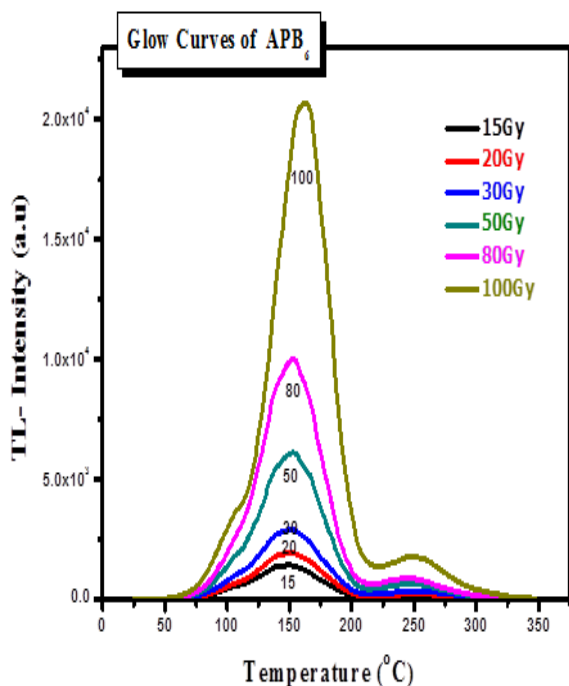


Fig. (6): Characteristic glow curves of APB<sub>6</sub> at different gamma absorbed dose from 15 Gy to 100 Gy

### 3.1.5. Dose response curve of APB<sub>6</sub>

One of the important features of any dosimeter is its linearity relationship between the TL intensity and the absorbed dose Fig. (7) shows the dose response

relationship of the sample APB<sub>6</sub> within a dose range of 15-100 Gy, where a linear response is obtained with .0.9925 correlation coefficient. In addition, the uncertainty percentage in integral intensity of APB<sub>6</sub> is within range of ± 3-20%. This behavior offers a good performance of using such new prepared nanophosphor materials in various fields of gamma measurements within the studied dose range.

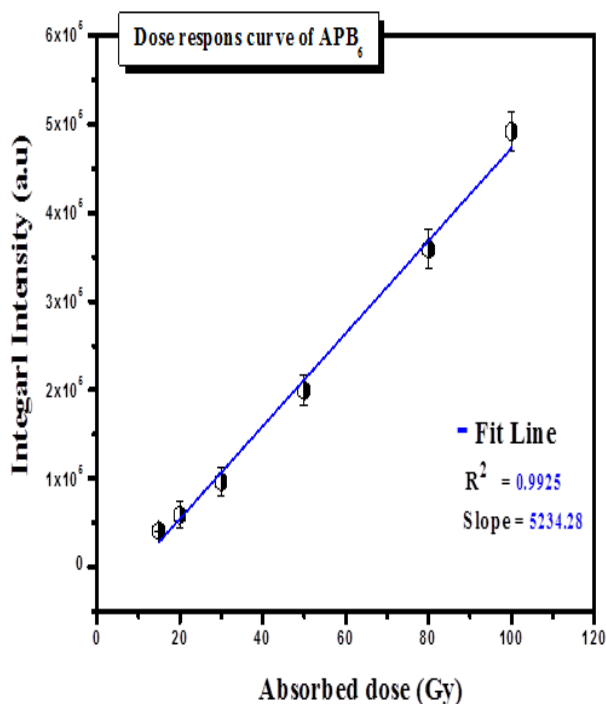


Fig. (7): TL response of APB<sub>6</sub> nanophosphors as a function of  $\gamma$ - doses

### 3.1.6. Minimum detectable dose

The minimum detectable dose (MDD) of synthesized APB<sub>6</sub> nanophosphor was determined by calculating the averaged TL signal B of 10 unirradiated chips (zero-dose) and the standard deviation of the average background  $\sigma$  to be substituted in the following equation [31]:

$$\text{MDD} = (B + 2\sigma) F \quad (1)$$

Where F is the calibration factor (Gy/TL). The MDD of the APB<sub>6</sub> sample was found to be about 247 mGy when region of interest was used. TLDs are generally employed to assess the high dose radiation (10Gy – 10kGy) from food sterilization, nuclear reactor and materials testing [32]. The linearity behavior range and MDD value of APB<sub>6</sub> sample offers the preference of using this nanophosphor material as food irradiation dosimeter [33]. However,

the use of conventional TLDs in these dose regimes can be limited due to the onset of saturation behavior of the TL response [34].

### 3.1.7. Test of batch size homogeneity

The recommendation of the International Electrochemical Commission (IEC) is that, the evaluated value for any dosimeter in a batch should not differ from any other dosimeter values, in the same batch by more than 30% [35].

This has been verified for the APB<sub>6</sub> nanophosphor sample with optimum conditions by irradiating 100 mg of the sample with 50 Gy of  $\gamma$ -dose by Co-60 source. The uniformity indice ( $\Delta$ ) were measured according to Eq. (2):

$$\Delta = (M_{\max} - M_{\min}) / M_{\min} \times 100 = 27.24\% \quad (2)$$

Where, max and min represent the maximal and minimal recorded values of TL-intensity, respectively. So that, the calculated value of ( $\Delta$ ) was 27.2%, which is lower than upper limit recommended by IEC. This shows the homogeneity of APB<sub>6</sub> sample used.

### 3.1.8. TL- stability of APB<sub>6</sub>

Fading is an important parameter and should be determined before the use of any TLD. It represents the loss of TL signal during the storage time. Samples of APB<sub>6</sub> phosphors were irradiated at 50 Gy  $\gamma$ -dose, then they were stored under dark conditions at room temperature and their TL was recorded at differ storage times over a period of 50 days. Each TL reading was normalized to that of zero storage time. Fig. (8) shows the relative TL response of APB<sub>6</sub> nanophosphor as a function of storage time (where  $F_0$  is the first read out intensity and  $F$  is the intensity at each interval). It is seen from Fig (8) that TL signals losses of 17% and 23% are detected after storage times 3 d and 16 d respectively. Afterwards, almost no losses were noticed for times higher than 23 days of storage. From the dosimetric point of view, these fading results should be considered in the evaluation of corrected  $\gamma$ -dose.

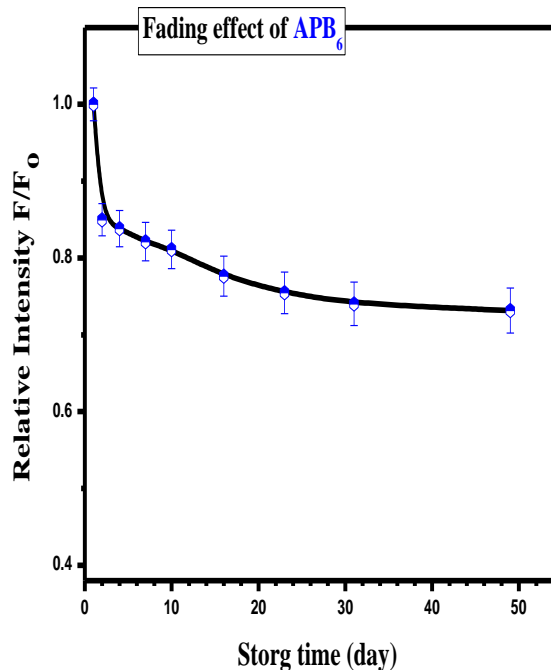


Fig. (8): The relative TL-response ( $F/F_0$ ) of the APB<sub>6</sub> sample as a function of storage time after irradiation with 50 Gy of  $\gamma$ -ray dose

## 3.2. Characterization

### 3.2.1. XRD analysis

The crystalline structure and phase composition of the as synthesized AP and APB<sub>6</sub> nanocrystalline samples were confirmed by XRD pattern as shown in Fig. (9). The pure (AP) sample exhibited the main peaks at [20.37°, 29.32°, 32.90°, 36.25°, 47.89°, 52.37° and 54.60°] which corresponds to plans (110), (200), (210),(211), (220),(310) and (222), that indexed to the pure body-centered cubic structure of (AP) according to the standard spectrum JCDPs No. (01-089-7399) as shown in Fig.9 (b,c).

In addition, the XRD patterns of the Ag<sub>3</sub>PO<sub>4</sub>.Ba<sup>2+</sup> (APB<sub>6</sub>) nanophosphor is shown in Fig.9 (a). The diffraction peaks at 2 $\theta$  position [20.03°, 21.86°, 26.36°, 27.63°, 30.59°, 31.85°, 32.72°, 38.45°, 39.05°, 43.55°, 44.85°, 45.85°, 49.8°, 55.85° and 56.85°] of the synthesized material were indexed by comparing them with the standard data available JCDPs No. (00-033-16167) which confirmed the successful synthesis of high crystalline AgBa(PO<sub>3</sub>)<sub>3</sub> nanocompound, without observing of other impurity diffraction peaks.

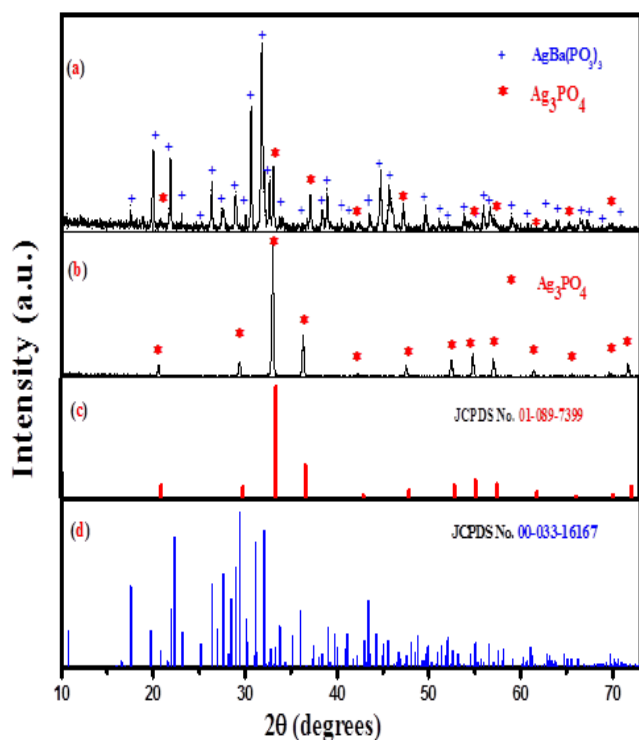
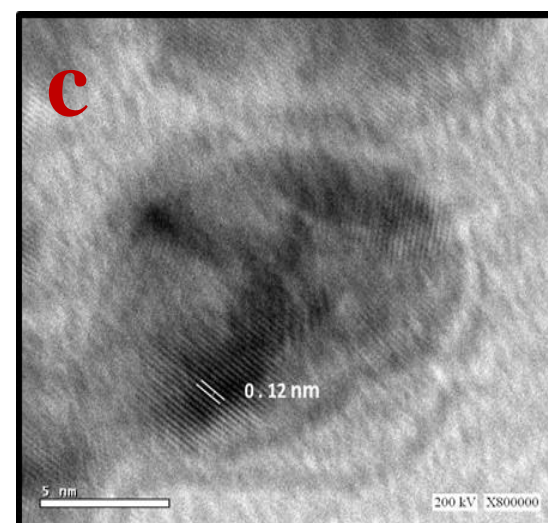
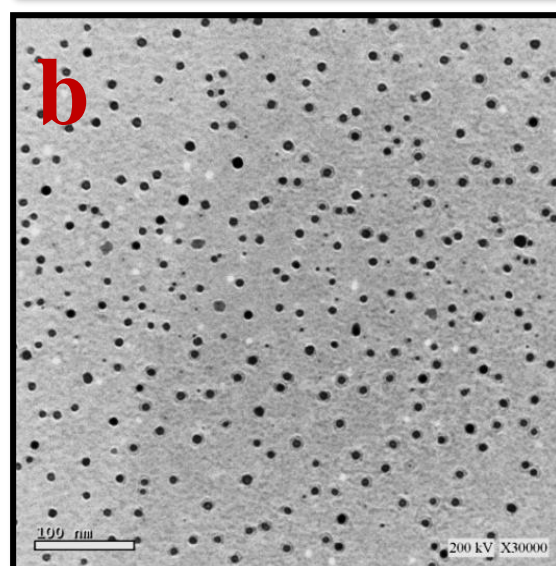
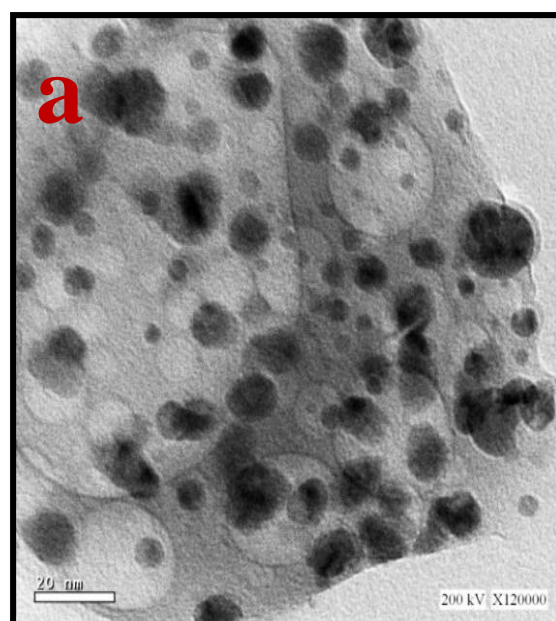


Fig. (9): The powder X-ray diffraction patterns of (a)  $\text{Ag}_3\text{PO}_4:\text{Ba}^{2+}$  ( $\text{APB}_6$ ), (b) undoped  $\text{Ag}_3\text{PO}_4$  (AP), (c)  $\text{Ag}_3\text{PO}_4$  - JCPDS card and (d)  $\text{AgBa}(\text{PO}_3)_3$  - JCPDS card

### 3.2.2. HR-TEM Analysis

Fig. (10) shows the morphological characterizations of the pure  $\text{Ag}_3\text{PO}_4$  and  $\text{Ag}_3\text{PO}_4:\text{Ba}^{2+}$  nanocrystalline samples by HR-TEM technique. Fig. 10(a) presents the representative TEM micrograph of pure (AP) NPs, with a uniform size of about 10 nm.

Fig. 10(b) depicts TEM image that confirmed the successful preparation of ( $\text{APB}_6$ ) NCs, by homogenized coprecipitation method, with average size of 20 nm. The TEM images in Fig. 10(c & d) show that all of the fine nanoparticles in the sphere exhibit clear lattice fringes with (d) spacing of 0.12 and 0.17 nm for the AP and  $\text{APB}_6$  samples respectively. This is considered a good agreement with the spacing of (220) and (200) planes of the cubic silver orthophosphate that confirmed the doping of  $\text{Ag}_3\text{PO}_4$  with  $\text{Ba}^{2+}$  ions. The corresponding *selected area electron diffraction* (SAED) images in Fig. 10(e & f) present a spot pattern for (AP) NPs that indicated a single-crystalline phase, and a rings pattern for ( $\text{APB}_6$ ) which showed a poly-crystalline phase.



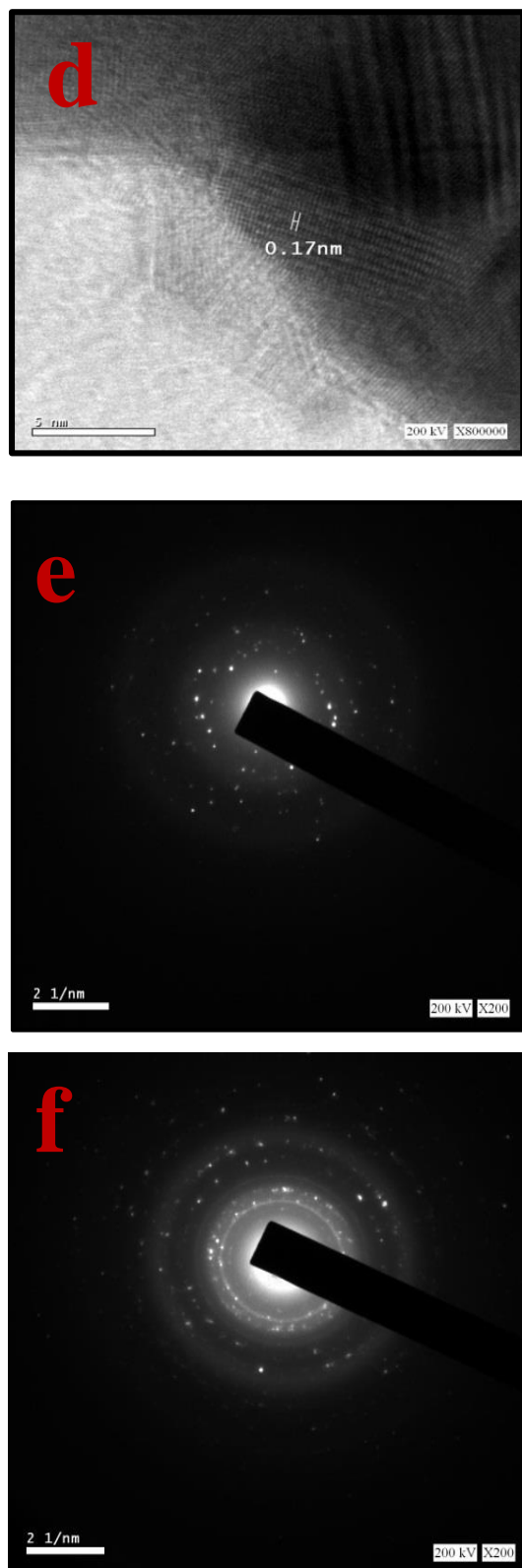


Fig. (10): (a,b) HR-TEM images of the as-prepared [AP and APB<sub>6</sub>] and their lattice fringes (c,d) and SAED images (e,f) respectively

#### 4. Conclusions

New nanostructure of barium Ba<sup>2+</sup> activated silver orthophosphate was synthesized by coprecipitation method with different Ba<sup>2+</sup> concentrations. The crystalline features of the prepared samples were confirmed via XRD and HR-TEM techniques. The TL properties of the prepared samples showed that the sample doped with 6 wt% of Ba<sup>2+</sup> impurity (i.e. APB<sub>6</sub> sample) and thermally annealed at 500 °C for 1h displayed the highest TL intensity among all the other compositions. The glow curve of APB<sub>6</sub> nanophosphor, recorded at 5°C/s heating rate displayed a simple structure having two peaks one strong prominent peak at about 151°C and second less intense peak center at about 249 °C. The TL characterizations of APB<sub>6</sub> sample revealed good linear gamma-dose ( $R^2 = 0.9925$ ) over a range from 15 to 100 Gy with low fading and good reproducibility. These excellent properties of the Ag<sub>3</sub>PO<sub>4</sub>:Ba<sup>2+</sup> nanophosphor sample offer the preference of using this novel synthesized nanophosphor material in various photonic dosimetric applications as gamma radiation detector.

#### 5- References

- [1] H. Hafez, E. Sheha, K. Abd-Elmageed, M. El-Kolaly, M. Sayed, The TL-properties of some environmental materials and assessment the effects of other different parameters, *Silicon*, 12 (2020) 1441-1448.
- [2] Gupta, P., Bedyal, A.K., Kumar, V., Singh, V.K., Khajuria, Y., Ntwaeaborwa, O.M. and Swart, H.C., Thermoluminescence and glow curves analysis of  $\gamma$ -exposed Eu<sup>3+</sup> doped K<sub>3</sub>Y (PO<sub>4</sub>)<sub>2</sub> nanophosphors. *Materials Research Bulletin*, 73, pp.111-118(2016).
- [3] Sahare, P.D., Bakare, J.S., Dhole, S.D. and Kumar, P., Effect of phase transition and particle size on thermoluminescence characteristics of nanocrystalline K<sub>2</sub>Ca<sub>2</sub> (SO<sub>4</sub>)<sub>3</sub>: Cu<sup>+</sup> phosphor. *Radiation Measurements*, 47(11-12), pp.1083-1091(2012).
- [4] Daniels, F., Boyd, C.A. and Saunders, D.F., Thermoluminescence as a research tool. *Science*, 117(3040), pp.343-349(1953).
- [5] Zhang, M., Liang, Y., Tong, M., Wang, Q., Yu, D., Zhao, J. and Wu, J. Photoluminescence properties and energy transfer of a novel bluish-green tunable K<sub>3</sub>SrY (PO<sub>4</sub>)<sub>2</sub>: Ce<sup>3+</sup>, Tb<sup>3+</sup> phosphor. *Ceramics International*, 40(7), pp.10407-10413(2014).
- [6] Du, Panpan, Siyuan Li, Xuejiao Wang, Qi Zhu, and Ji-Guang Li. "On the role of Zr substitution in structure modification and photoluminescence of Li<sup>5+</sup>2<sub>x</sub>La<sub>3</sub>(Ta<sub>1</sub>-

- $x\text{Zr}_x\text{O}_{12}:\text{Eu}$  garnet phosphor." *Dalton Transactions* (2021).
- [7] Gieszczyk, W., Bilski, P., Kłosowski, M., Nowak, T. and Malinowski, L., Thermoluminescent response of differently doped lithium magnesium phosphate ( $\text{LiMgPO}_4$ , LMP) crystals to protons, neutrons and alpha particles. *Radiation Measurements*, 113, pp.14-19(2018).
- [8] Pardhi, S.A., Nair, G.B., Sharma, R. and Dhoble, S.J., Investigation of thermoluminescence and electron-vibrational interaction parameters in  $\text{SrAl}_2\text{O}_4:\text{Eu}^{2+}, \text{Dy}^{3+}$  phosphors. *Journal of Luminescence*, 187, pp.492-498(2017).
- [9] Phuruangrat, A., Aon-on, P., Thongtem, T. and Thongtem, S., Synthesis and photocatalysis of  $\text{Ag}_3\text{PO}_4$  nanoparticles loaded on ZnO nanostructure flowers. *Journal of the Australian Ceramic Society*, 55(4), pp.1147-1152.8(2019).
- [10] Zeler, J., Bolek, P., Kulesza, D. and Zych, E., On thermoluminescence mechanism and energy leakage in  $\text{Lu}_2\text{O}_3:\text{Tb}, \text{V}$  storage phosphor. *Optical Materials: X*, 1, p.100001(2019).
- [11] Salah, N., Alharbi, N.D., Habib, S.S. and Lochab, S.P., Luminescence properties of  $\text{CaF}_2$  nanostructure activated by different elements. *Journal of Nanomaterials*, (2015).
- [12] Li, X., Xu, P., Chen, M., Zeng, G., Wang, D., Chen, F., Tang, W., Chen, C., Zhang, C. and Tan, X., Application of silver phosphate-based photocatalysts: Barriers and solutions. *Chemical Engineering Journal*, 366, pp.339-357(2019).
- [13] Zhong, K. and Su, J., Study on the visible-light photocatalytic performance of  $\text{Ag}_3\text{PO}_4/\text{Cu}_2\text{O}$  composite. *Research on Chemical Intermediates*, 45(3), pp.1207-1216(2019).
- [14] Septiarini, D.A., Kurniasih, M., Andreas, R., Hermawan, D. and Sulaeman, U., April. Synthesis of silver orthophosphate under dimethyl sulfoxide solvent and their photocatalytic properties. In IOP Conference Series: *Materials Science and Engineering* (Vol. 509, No. 1, p. 012151). *IOP Publishing* (2019).
- [15] Hou, G., Zeng, X. and Gao, S., Fabrication and photocatalytic activity of core@ shell  $\text{Ag}_3\text{PO}_4@\text{Cu}_2\text{O}$  heterojunction. *Materials Letters*, 238, pp.116-120(2019).
- [16] He, G., Yang, W., Zheng, W., Gong, L., Wang, X., An, Y. and Tian, M., Facile controlled synthesis of  $\text{Ag}_3\text{PO}_4$  with various morphologies for enhanced photocatalytic oxygen evolution from water splitting. *RSC Advances*, 9(32), pp.18222-18231(2019).
- [17] Afif, M., Sulaeman, U., Riapanitra, A., Andreas, R. and Yin, S., Use of Mn doping to suppress defect sites in  $\text{Ag}_3\text{PO}_4$ : Applications in photocatalysis. *Applied Surface Science*, 466, pp.352-357(2019).
- [18] Zhao, X., Song, L. and Zhang, S., Synthesis of  $\text{AgCl}/\text{Ag}_3\text{PO}_4$  composite photocatalysts and study on photodegradation activity based on a continuous reactor. *Photochemistry and Photobiology*, 94(3), pp.484-490 (2018).
- [19] Song, Z. and Y. He, Hydrothermal Synthesis of heterostructured  $\text{Ag}_3\text{PO}_4/\text{TiO}_2$  photocatalyst with enhanced photocatalytic activity and stability under visible light. *Digest Journal of Nanomaterials and Biostructures*, 12(1): p. 151-158(2017).
- [20] Song, X., Li, R., Xiang, M., Hong, S., Yao, K. and Huang, Y., Morphology and photodegradation performance of  $\text{Ag}_3\text{PO}_4$  prepared by  $(\text{NH}_4)_3\text{PO}_4, (\text{NH}_4)_2\text{HPO}_4$  and  $\text{NH}_4\text{H}_2\text{PO}_4$ . *Ceramics International*, 43(5), pp.4692-4701(2017).
- [21] Rajammal, K., Sivakumar, D., Duraisamy, N., Ramesh, K. and Ramesh, S., Na-doped  $\text{LiMnPO}_4$  as an electrode material for enhanced lithium ion batteries. *Bulletin of Materials Science*, 40(1), pp.171-175 (2017).
- [22] Chava, R.K., Do, J.Y. and Kang, M., Fabrication of  $\text{CdS}-\text{Ag}_3\text{PO}_4$  heteronanostructures for improved visible photocatalytic hydrogen evolution. *Journal of Alloys and Compounds*, 727, pp.86-93(2017).
- [23] Kumar, A., Kumar, A., Dogra, R., Manhas, M., Sharma, S. and Kumar, R., Investigation of thermoluminescence and kinetic parameters of gamma ray exposed  $\text{LiF}:\text{Sm}^{3+}, \text{Eu}^{3+}$  nanophosphors for dosimetric applications. *Ceramics International*, 44(13), pp.15535-15541(2018).
- [24] Qin, L., Tao, P., Zhou, X., Pang, Q., Liang, C., Liu, K. and Luo, X., Synthesis and characterization of high efficiency and stable spherical  $\text{Ag}_3\text{PO}_4$  visible light photocatalyst for the degradation of methylene blue solutions. *Journal of Nanomaterials*, (2015).
- [25] Huang, K., Lv, Y., Zhang, W., Sun, S., Yang, B., Chi, F., Ran, S. and Liu, X., One-step synthesis of  $\text{Ag}_3\text{PO}_4/\text{Ag}$  photocatalyst with visible-light photocatalytic activity. *Materials Research*, 18(5), pp.939-945(2015).
- [26] Cao, M., Wang, P., Ao, Y., Wang, C., Hou, J. and Qian, J., Preparation of graphene oxide-loaded  $\text{Ag}_3\text{PO}_4@\text{AgCl}$  and its photocatalytic degradation of methylene blue and  $\text{O}_2$  evolution activity under visible light irradiation. *International Journal Of Hydrogen Energy*, 40(2), pp.1016-1025(2015).
- [27] Bozetine, I., Boukennous, Y., Trari, M. and Moudir, N., Synthesis and characterization of orthophosphate silver powders. *Energy Procedia*, 36, pp.1158-1167(2013).
- [28] Amornpitoksuk, P., Intarasuwan, K., Suwanboon, S. and Baltrusaitis, J., Effect of phosphate salts ( $\text{Na}_3\text{PO}_4, \text{Na}_2\text{HPO}_4$ , and  $\text{NaH}_2\text{PO}_4$ ) on  $\text{Ag}_3\text{PO}_4$  morphology for photocatalytic dye degradation under visible light and toxicity of the degraded dye products. *Industrial & Engineering Chemistry Research*, 52(49), pp.17369-17375(2013).

- 
- [29] Ju, G., Hu, Y., Chen, L., Wang, X. and Mu, Z., Concentration quenching of persistent luminescence. *Physica B: Condensed Matter*, 415, pp.1-4(2013).
- [30] Wang, L., Dai, Z., Zhou, R., Qu, B. and Zeng, X.C., Understanding the quenching nature of Mn<sup>4+</sup> in wide band gap inorganic compounds: design principles for Mn<sup>4+</sup> phosphors with higher efficiency. *Physical Chemistry Chemical Physics*, 20(25), pp.16992-16999 (2018).
- [31] Oguz, Kemal Firat, and Mehmet Yüksel. "Determination Of The Minimum Detectable Dose And The Effect Of Different Filters On The Tld-100h 260 C Thermoluminescence Peak." *RAP Conference Proceedings*, vol. 4, pp. 136–138, (2020).
- [32] Roberson, Peter L., and R. Douglas Carlson. "Determining the lower limit of detection for personnel dosimetry systems." *Health physics* 62, no. 1 (1992)
- [33] Dosimetry for Food Irradiation, IAEA, Vienna, 2002, Technical Reports Series No. 409" (PDF). Retrieved March 19, (2014).
- [34] Meireles, Leonardo S., Marco Aurelio S. Lacerda, Luiz C. Meira-Belo, and Hudson R. Ferreira. "Study of the influence of the time temperature profile on the minimum detectable dose of TLD-100." (2013).
- [35] Stefanik, J., Thermoluminescence dosimetry systems for personal and environmental monitoring, International Electrotechnical Commission Standard Publication 61066:1991 (2000).